2019 SECED Conference
Earthquake risk and engineering towards a resilient world
9-10 September 2019, Greenwich, London

TIME-DEPENDENT SEISMIC RISK OF REGULAR HIGHWAY BRIDGES UNDER THE EFFECT OF STRUCTURAL DETERIORATION

Taner YILMAZ[1] & Onur Cem AYGIN[2]

Abstract: *The importance of sustainable and resilient infrastructure systems has increased significantly in recent years due to the need for the transportation systems with minimum interruptions under extreme events. To reach this objective, it is crucial to evaluate the lifetime performance of bridges that are affected from both the factors associated with structural response and the demands induced by hazard conditions. Bridge fragilities at different performance levels and associated bridge risks may increase in time owing to the structural deterioration effects on different bridge components. The present study aims to obtain the time-dependent fragility and risk of regular highway bridges under the combined deterioration effects on bridge piers and on elastomeric bearings. For this purpose, the seismic response of a characteristic river-crossing highway bridge is investigated and the physical models reflecting the structural deterioration are incorporated into the developed three-dimensional bridge models for different time instants along the bridge lifetime. Fragility curves at component and system levels are generated by performing a large number of nonlinear time-history analyses. The computed time-dependent fragilities are further employed to obtain time-dependent risk curves of the study bridge. The outcomes of the study can be utilized in future efforts towards decision-making methodologies in risk-mitigation and maintenance planning studies.*

Introduction

The objective of achieving sustainable and resilient highway transportation systems requires the life time risk assessment of bridges that are affected from both the factors associated with structural response and the demands induced by multiple hazard conditions. Performance of bridge components may downgrade in time as a result of several deterioration and aging effects, hence bridges may become more vulnerable than their initial state against earthquakes. For example, elastomers can be exposed to various aging mechanisms and their stiffness can be considerably affected by thermal oxidation deterioration (Itoh et al. 2006). Highway bridges located near seashores or at places having tough winter conditions experience deterioration of steel reinforcement in reinforced concrete (RC) piers due to chloride-induced corrosion as a result of marine exposure or the usage of deicing salts. This can mainly affect the bridge performance due to the reduction in steel reinforcement area (Cui, 2016). Within the present study, the time-dependent seismic risk of characteristic highway bridges is investigated under the combined chloride-induced corrosion effects on RC piers and thermal oxidation of rubber pads at bearings.

Most of the past research investigating the time-dependent seismic performance of aging bridges explored the effect of chloride-induced corrosion effects on several bridge components especially on RC bridge columns. Enright and Frangopol (1998) and Stewart and Rosowsky (1998) investigated the strength loss of bridge RC elements due to chloride-induced corrosion of steel reinforcement either from deicing salt application or atmospheric exposure in marine environment while assuming a uniform pattern for steel area loss. Hoeke et al. (2009) studied the effects of corrosion deterioration on the performance of steel bearings of bridges. Ghosh and Padgett (2010) evaluated the joint impact of chloride-induced corrosion of RC columns and steel bridge bearings on the seismic fragility of multi-span continuous highway bridges and they concluded that the seismic fragility of the most critical components and system-level fragility is increased over time due to corrosion. Gardoni and Rosowsky (2011) proposed incremental fragility functions for bridges subject to corrosion. Ghosh and Sood (2016) implemented improved capacity limit state definitions to their fragility framework which accounts for capacity degradation due pitting

[1] Assistant Professor, Ozyegin University, Istanbul, Turkey, taner.yilmaz@ozyegin.edu.tr
[2] M.Sc. student, Ozyegin University, Istanbul, Turkey,

corrosion. Shekhar et al. (2018) determined the life-cycle cost of a bridge that is subject to different chloride exposure conditions and proposed various improvements to the corrosion deterioration model.

Despite the remarkable findings of the previous literature on the subject, there is still a lack of studies investigating the seismic performance of bridges subject to the deterioration of bridge components other than the chloride-induced corrosion at piers. Also, the time-dependent seismic performance assessment is generally kept at the level of fragility curves, while the impact of deterioration effects on bridge risk under various hazard levels has not been adequately addressed. Thus, this study aims to evaluate the combined effect of pier and bearing deterioration on time-dependent seismic fragility and risk of aging bridges.

Methodology

In order to obtain the time-varying seismic fragility characteristics of aging bridges, a three-span characteristic bridge depicted in Figure 1 is taken as the study bridge. The superstructure of the bridge comprises a continuous concrete box girder resting on seat-type abutments. Each bent is composed of two RC piers extending below ground as pile shafts. This generic bridge was previously derived after an inventory study of the bridges in the West of the U.S. for assessment of multi-hazard risk of highway bridges under flood-induced scour and earthquake (Yilmaz and Banerjee, 2018). Seismic analyses of the study bridge are performed incorporating the considered deterioration effects at several instants throughout the life time of the bridge. The deterioration effects are adopted from the physical models for chloride-induced corrosion in RC columns and thermal oxidation in elastomeric bearings based on the existing literature. Expected (mean) values of the input parameters are utilized for both the bridge modelling parameters and the parameters describing the physical deterioration models.

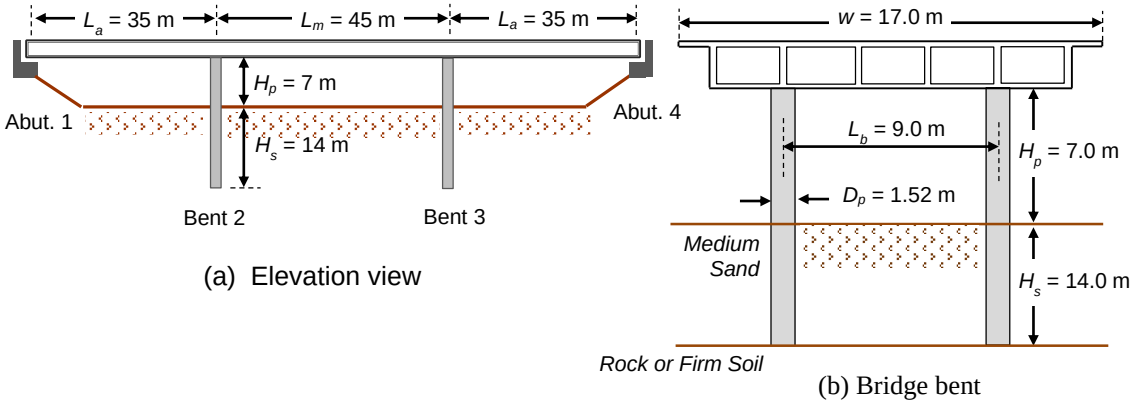

Figure 1. Schematic drawing of the study bridge.

Chloride-Induced Corrosion in RC Piers

This study considers the influence of corrosion on only RC piers and any probable effect of corrosion on other bridge components (e.g. girders) is neglected in analyses. The assessment of the effect of corrosion on RC columns have been investigated in previous studies for various environmental exposure conditions. Some of these studies focused on the corrosion attack from the application of chloride-laden deicing salts (Ghosh and Padgett, 2010), while some others considered marine environment exposure conditions such as atmospheric, splash and tidal and submerged zones (Guo et al. 2015). The present study assumes moderate level of chloride exposure condition which can be thought of representing marine environment condition as described in Ghosh and Sood (2016).

The primary effect of chloride-induced corrosion on RC piers is the loss of reinforcing steel areas as the rust produced by metal-chloride reaction gradually replaces the steel material. Many studies on seismic fragility assessment of bridges accepted uniform deterioration of reinforcing steel areas along the bar length, yet consideration of localized corrosion pits (pitting corrosion) in addition to the uniform reduction of steel area was also proposed by Ghosh and Padgett (2010).

This study adopts the implementation of uniform reinforcement area loss as proposed by Vu and Stewart (2000) due to the uncertainties in determining the location of pitting corrosion. Besides the reduction of longitudinal and transverse steel reinforcement areas, some researchers also investigated the secondary effect of reduced compressive strength of cover concrete and reduction in yield strength of reinforcing bars (Guo et al, 2015) during the corrosion process. Within the scope of this study, secondary effects of chloride-induced corrosion are neglected and the only focus is on the primary effect of reduction in longitudinal reinforcement area and the degradation in the confined concrete compressive strength due the reduction in transverse reinforcement area as presented in the framework by Shekhar et al. (2018).

There are several factors in the defining the corrosion process in RC piers. Corrosion initiation time (T_i) is the time required for chloride ions to diffuse through the concrete cover, penetrate through passivation later and initiate corrosion (Ghosh and Sood, 2016). For marine environment, corrosion initiation time can be determined using the following equation as proposed by Duracrete (2000):

$$T_i = \left\{ \frac{x^2}{4 k_e k_c D_{cl,0} (t_0)^{n_{cl}}} \left[erf^{-1}\left(\frac{C_s - C_{cr}}{C_s} \right) \right]^{-2} \right\}^{\frac{1}{(1-n_{cl})}} \quad (1)$$

where x is the concrete cover (in mm), k_e is the environmental factor, k_c is the curing factor, $D_{cl,0}$ is the reference diffusion coefficient (in mm^2/year) determined from compliance tests, t_0 is the age of the concrete at which the compliance test is performed, n_{cl} is the age exponent which accounts for the densification of cement paste, C_s is the equilibrium chloride concentration at the concrete surface, C_{cr} is the critical chloride concentration, and *erf* is the Gaussion error function. Assuming uniform corrosion of steel, the diameter of the reinforcing bars at time t can be calculated as:

$$D(t) = D_0 - r_{corr}(t - T_i) \quad (2)$$

where D_0 is the initial bar diameter, r_{corr} is the corrosion rate (in mm/year), t is the age of the structure and T_i is the corrosion initiation time. Corrosion rate which is assumed to be not varying with time can be calculated as:

$$r_{corr} = 0.0116 \frac{37.8\left(1 - \frac{w}{c}\right)^{-1.64}}{x} \quad (3)$$

where *w/c* is the water to cement ratio of concrete. The values of the parameters used in calculation of corrosion initiation time and the corrosion rate are presented in Table 1.

Parameter	Unit	Value
x	(mm)	50
k_e		0.265
k_c		1.5
$D_{cl,0}$	(mm^2/year)	473
t_0	(year)	0.077
n_{cl}		0.362
C_s	(by weight %)	3.879
C_{cr}	(by weight %)	0.5
T_i	(year)	**22.7**
r_{corr}	(mm/year)	**0.0273**

Table 1. Utilized chloride-induced corrosion parameters

Load carrying capacity and the ductility of a RC bridge piers is not only affected from the decrease in the cross-sectional area of longitudinal reinforcement, but also from the reduction in the

confinement pressure as a result of the decrease in the cross-sectional area of lateral reinforcement. Figure 2 shows the change in moment-curvature of a bridge column under an axial load level of $N = 0.1 f_c A_c$ for pristine condition and for structure ages of 25, 50, 75 and 100 years. This figure reveals that the moment capacity and the ductility capacity of the bridge column decay with time as a result of the reduced longitudinal and lateral steel areas.

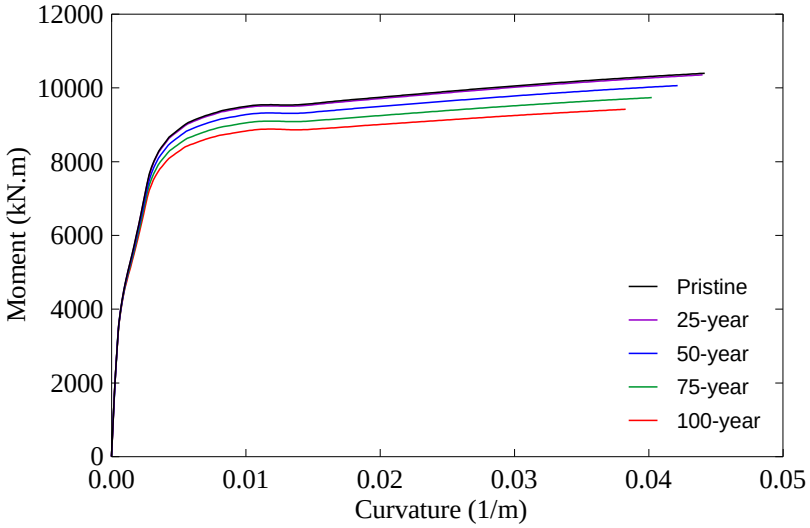

Figure 2. Moment-curvature of a pier for pristine condition and different ages.

Thermal Oxidation of Elastomeric Bearings

Performance of elastomeric bearings can be predominantly affected by thermal oxidation phenomenon (Itoh et al. 2006) as their horizontal stiffness is increased due to thermal oxidation (Itoh and Gu, 2009). Rubber pad material starts to show a spontaneous reaction from the very early stages of aging and this reaction reaches equilibrium point after a certain time. In the present study, the rubber material is assumed to reach its equilibrium state in 20 years following the recommendation of Paramashanti et al. (2007). Time-dependent shear modulus of the elastomeric bearing is determined from the following equation (Paramashanti et al. 2007):

$$G(t) = G_0\left[\left(a-2d^*\right)\left(b-2d^*\right)+2d^*\left(a+b-4d^*\right)\left(1+\Delta f_s/3\right)+4d^{*2}\left(1+\Delta f_s/2\right)\right]\cdot\left(1+\Delta f_i\right) \quad (4)$$

where G_0 is the initial shear modulus, a and b are the dimensions of the elastomeric bearing and d^* is the critical depth of oxidation. Δf_i and Δf_s account for the rate of change in shear modulus due to spontaneous reaction and oxidation, respectively and could be calculated from the following equations:

$$\Delta f_i = 88.4\exp\left(\frac{-1887.2}{T}\right) \quad (5)$$

$$\Delta f_s = 0.93\times10^{-4}\, t_{ref} \quad (6)$$

where T is the absolute temperature in service condition and t_{ref} is the equivalent aging time at the reference temperature, which can be determined from the following equation:

$$\ln\left(\frac{t_{ref}}{t}\right) = \frac{E_a}{R}\left(\frac{1}{T_{ref}}-\frac{1}{T}\right) \quad (7)$$

where t is the real aging time, E_a is the activation energy of the rubber pad, R is the gaseous constant and T_{ref} is the reference temperature of the accelerated thermal oxidation test. The

parameters employed for thermal oxidation are summarized in Table 2 and the time-varying shear modulus of elastomer is presented in Figure 3.

Parameter	Unit	Value
T_{ref}	(K)	288
T	(K)	343
E_a	(10^4 J/mol)	9.04
R	(J/mol/K)	8.31
α	(10^{-4} mm)	1.20
β	(10^3 K^{-1})	3.82
d^*	(mm)	78.4
G_0	(kN/m^2)	741.4

Table 2. Utilized thermal-oxidation parameters for elastomeric bearings

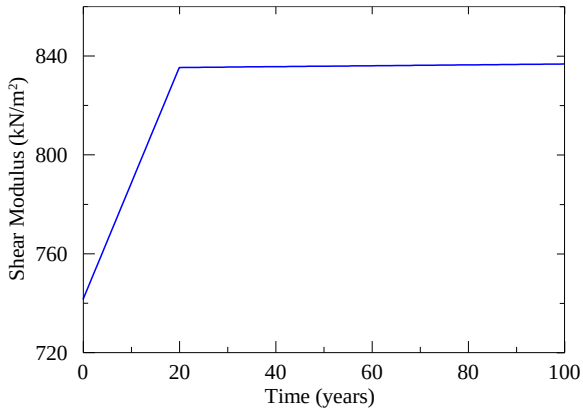

Figure 3. The change in shear modulus of elastomer at different ages.

Fragility Analysis

Three dimensional finite element (FE) models of the study bridge at different ages (including the pristine condition) are generated in the FE simulation platform OpenSees (McKenna and Fenves, 2012). Linear elastic beam-column elements with equivalent mass and stiffness properties lumped at the center of the members are used to model the bridge girder. Piers and shafts are modeled with nonlinear fiber elements employing the concrete material model of Mander et al. (1998). The dynamic response of abutments, bearings and shear keys are represented with several nonlinear components in the bridge model. Elastoplastic elements with a gap property are utilized to model the abutment backwall response in the longitudinal direction accounting for the expansion joints at both ends of the bridge. The backbone curve of the abutment backwall in the longitudinal direction is taken as described in Caltrans (2013), while for the transverse direction the response in longitudinal direction is modified as recommended by Aviram et al. (2008). Abutment bearings are represented with elastoplastic elements in both two horizontal directions and with linear elements in the vertical direction and for rotation about the transverse axis. Soil-structure interaction at the pile foundations is taken care of by a series of soil springs placed along the shafts and *p-y* curves are assigned onto these springs in two horizontal directions to reflect the nonlinear behavior of soil. Full fixity is applied at the bottom of piles which are assumed to be socketed into firm soil layers. The readers are referred to Yilmaz (2015) for the bridge modeling approach applied herein.

A large set of nonlinear time-history analyses are performed to generate the seismic fragility curves at component and system levels. The ground motion data set is formed by acquiring the corrected and filtered real ground motions from the Next Generation Attenuation (NGA) database of the Pacific Earthquake Engineering Research (PEER, 2019). In the process of computing seismic fragility curves, the damage states of critical bridge components (i.e. piers, abutments, bearings and shear keys) are determined based on the structural responses resulting from each time-history analysis. Four damage states (i.e. minor, moderate, major and collapse) as defined

in in HAZUS (2013) is taken into consideration where the threshold limits of engineering demand parameters for each damage state of the critical bridge components are specified based on a review of past studies. The details on the damage state limits could be found in Yilmaz (2015).

A two-parameter lognormal distribution as presented in Equation (8) can be used to define fragility curves (Shinozuka et al. 2003):

$$F\left(x_j, c_k(t), \zeta\right) = \Phi\left[\frac{\ln\left(\frac{x_j}{c_k(t)}\right)}{\zeta_k}\right] \tag{8}$$

where the fragility function $F()$ denotes the failure probability of a bridge component or the bridge system at a damage state k under a ground motion j with the peak ground acceleration (PGA) x_j. Fragility parameters, ζ and $c_k(t)$, refer to lognormal standard deviation and time-dependent median values for k^{th} damage state, respectively. The present study assumes a single value of ζ_k= 0.6 as given in HAZUS (2013) for all damage states in order to prevent the intersection of any two fragility curves so that fragility curves can be compared only according to their median values. The method of maximum likelihood is employed to get the median values (c_k) by using the damage state resulting from each time-history analysis. A lower median value denotes a higher failure probability of the bridge component (or the system). The system-level fragility curves are obtained such that the global damage state of the bridge is represented by the worst damage state amongst all critical bridge components.

Seismic Risk Analysis

A primitive risk analysis is carried out to estimate the time-dependent seismic risk of the study bridge subject to structural deterioration. For this purpose, seismic risk curves of the bridge are computed at different ages of the study bridge. A risk curve represents the annual exceedance probabilities of the negative consequences resulting from the occurrences of a range of earthquake levels. Various sources of socio-economic losses can be included into such consequences, however within the scope of the present study, only the bridge restoration cost following a seismic event is taken as the source of losses which can directly reflect the post-event performance reduction of the bridge. Bridge restoration cost (C_{Rm}) following a seismic event m can be obtained from (Zhou *et al*. 2010):

$$C_{Rm} = \sum_{k=1}^{4} p_m\left(k, x_m, t\right) C_n r_k \tag{9}$$

where $p_m(k, x_m, t)$ is the time-dependent probability that the bridge sustains the damage state k under a ground motion with PGA = x_m, which can be obtained from system-level seismic fragility curves of the bridge computed at different ages of the bridge. In Equation 9, C_n refers to the bridge total replacement cost and r_k is damage ratio for the damage state k, as recommended by HAZUS (2013).

The study bridge is assumed to be located in a seismic-prone region, thus the annual exceedance probabilities of a range of earthquake events at the bridge location is needed for computing the risk curve. Figure 4 depicts the mean seismic hazard curve of an investigated location (referred to as “Site 3”) in Yilmaz and Banerjee (2018) which is utilized here for the computation of the time-dependent seismic risk curves.

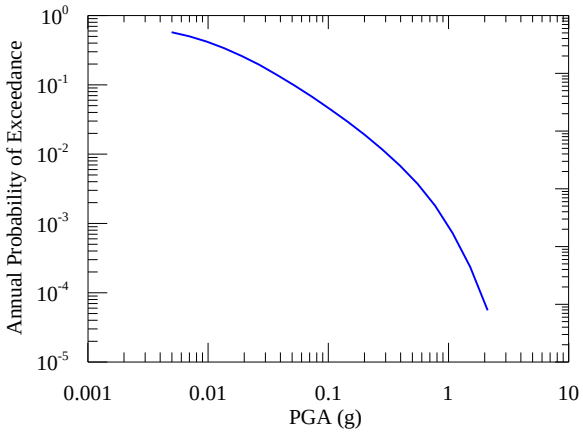

Figure 4. Seismic hazard curve accepted at the selected bridge location.

Results

Time-dependent seismic fragility curves developed for the most critical components, piers and bearings, under the presence of combined pier and bearing deterioration effects are presented in Figure 5. As can be observed from these curves, seismic performance of the piers worsen as the bridge gets older with a more gradual trend at lower damage states. On the hand, the fragility of bearings is increased at only moderate damage state after 25 years, while the deterioration does not have any influence on the performance of bearing at other damage states. Please note that some of the curves in Figure 5 are overlapped due to having the same fragility curve parameters. This is mainly due to the approach used for generating the fragility parameters. Figure 6 shows the time-dependent system-level seismic fragility curves of the bridge. It can be inferred from this figure that bearings govern the system-level fragilities at minor and moderate damage states, while piers control the fragilities at the higher damage states.

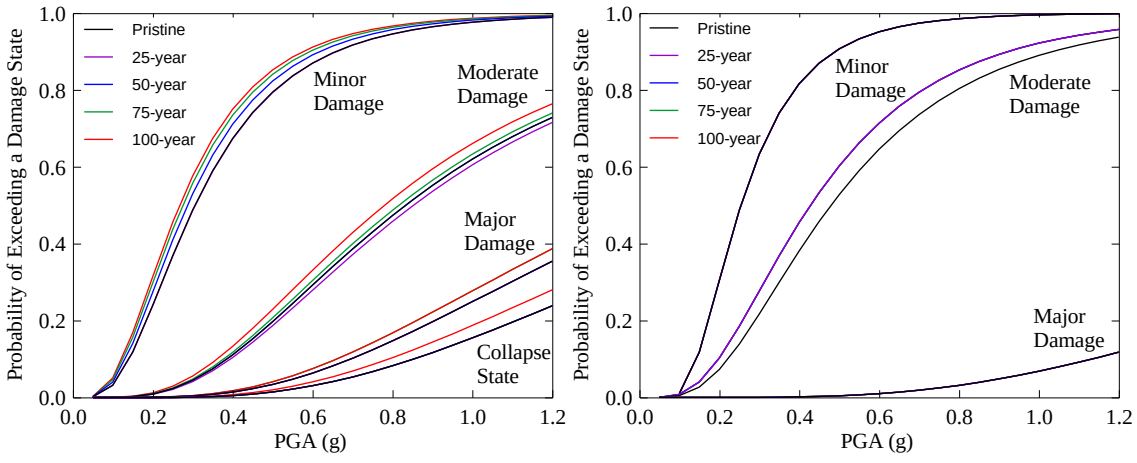

Figure 5. Seismic fragility curves of (a) piers and (b) bearings for different ages of the study bridge.

In order to observe the extent of the influence of the deterioration of elastomeric bearings due to thermal oxidation, time-dependent seismic fragility curves of the bridge without bearing deterioration are generated as well. Table 3 displays the median values of the fragility curves for piers that are obtained under the presence of combined deterioration of piers and bearings and under the presence of pier deterioration only. This table reveals that the deterioration in bearings has a minimum influence on the fragility characteristics of piers and it is limited only at low damage states. On the other hand, chloride-induced corrosion in RC piers is observed to have notable adverse impact on the seismic performance, while this effect exists for almost all damage states.

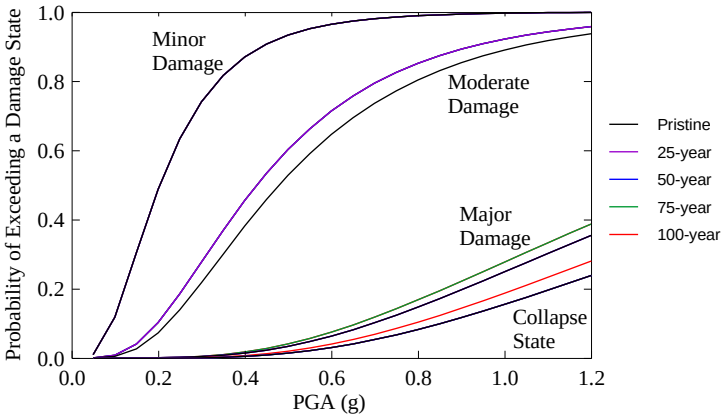

Figure 6. Seismic fragility curves of (a) piers and (b) bearings for different ages of the study bridge.

Age	Minor		Moderate		Major		Collapse	
	A	B	A	B	A	B	A	B
Pristine	0.305	0.305	0.833	0.833	1.502	1.502	1.834	1.834
25-year	0.306	0.301	0.853	0.833	1.502	1.502	1.834	1.834
50-year	0.287	0.283	0.833	0.833	1.502	1.502	1.834	1.834
75-year	0.275	0.275	0.816	0.816	1.427	1.427	1.834	1.834
100-year	0.267	0.263	0.780	0.816	1.427	1.427	1.699	1.699

Table 3. Median values of the seismic fragility curves for piers; A: Under the presence of combined deterioration of piers and bearings, B: Under the presence of pier deterioration only.

Figure 7 demonstrates the time-dependent risk curves of the bridge for the pristine condition and for different ages of the bridge. On this figure, the expected seismic losses can be evaluated in terms of the restoration cost (C_{Rm}) and also restoration to replacement cost ratio C_{Rm}/C_n. Please note that the risk calculations are made for the whole bridge using the system-level fragility curves as bridge components are not considered separately for the loss calculations. The overlapping risk curves for the pristine condition and the ones belonging to different ages reveal that the mean-level seismic risk of the bridge is not significantly affected from the presence of structural deterioration until the age of 75-years.

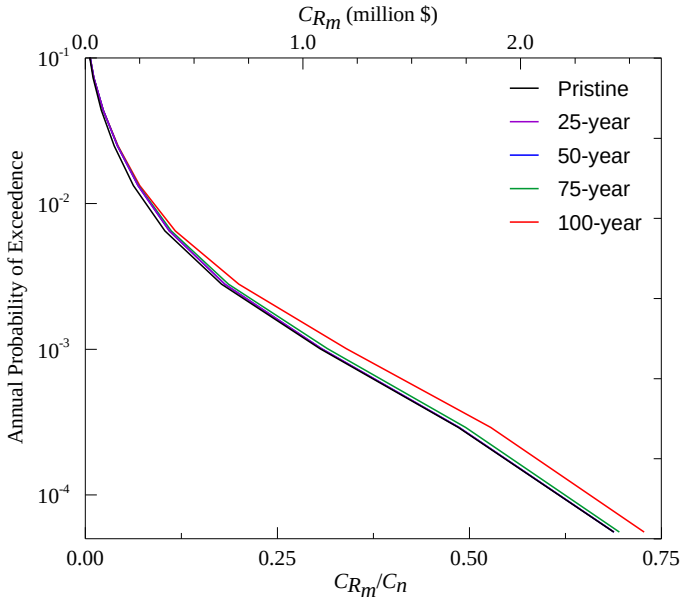

Figure 7. Time-dependent risk curves of the bridge.

Conclusions

This paper presents the outcomes of our research on seismic risk assessment of regular highway bridges under the effect of structural deterioration. Within the applied methodology, 3-D FE models of a characteristic regular highway bridge are generated incorporating the effects of physical deterioration models of piers and bearings at different ages. Nonlinear time-history analyses of the study bridge are performed to obtain time-dependent seismic fragility curves at component and system levels. In addition, time-dependent risk curves are computed using the produced fragility curves of the bridge for an assumed earthquake-prone location of which seismic hazard curve is available.

The results obtained from this study showed that aging bridges have the general trend of higher seismic fragility and risk in time because of structural deterioration effects. Another important conclusion is that chloride-induced corrosion at RC piers is the main contributing factor to the increased bridge fragilities and deterioration of bearings has a negligible influence on general bridge seismic performance. It can be also said that the increase in seismic risk of the bridge due to structural deterioration is well pronounced only after a certain age, particularly 75 years in this study. However, this conclusion is reached when the risk calculations are made based on the system-level fragility curves and this approach can be improved when fragilities of each critical component are separately considered.

The outcomes of this study reveal the importance of assessing the time-varying seismic fragility and risk of highway bridge due to structural deterioration of bridge components. The results obtained from this study can contribute to the knowledge base for future efforts in risk risk-mitigation and maintenance planning studies against earthquake hazards. For our future research, the framework presented here will be extended for the multi-hazard condition of flood-induced scour and earthquake and uncertainties in modeling, hazard and losses will be considered in detail.

Acknowledgements

This research was funded by the Turkish National Science and Technology Institute (Tübitak) through Grant No. 118M618.

References

Aviram A, Mackie KR and Stojadinovic B (2008). Effect of abutment modeling on the seismic response of bridge structures. *Earthquake Eng. &Eng. Vib.*, 7(4): 395–402.

Caltrans (2013). *Seismic design criteria, version 1.7*, California Department of Transportation, Sacramento, CA.

Cui Z (2016). *Lifetime performance prediction of reinforced concrete structures in multi-threat areas*, Ph.D. dissertation, Iowa State University, IA.

Duracrete (2000). *Probabilistic Performance-Based Durability Design of Concrete Structures: Final Technical Report*, The European Union – Brite EuRam III.

Enright MP and Frangopol DM (1998). Probabilistic analysis of resistance degradation of reinforced concrete bridge beams under corrosion, *Engineering Structures*, 20(11): 960-971.

Gardoni P and Rosowsky D (2011). Seismic fragility increment functions for deteriorating reinforced concrete bridges. *Structure and Infrastructure Engineering*. 7: 869-879.

Ghosh J and Padgett JE (2010). Aging considerations in the development of time-dependent seismic fragility curves, *J. Structural Engineering*, 136(12): 1497-1511.

Ghosh J and Sood P (2016). Consideration of time-evolving capacity distributions and improved degradation models for seismic fragility assessment of aging highway bridges. *Reliability Engineering and System Safety*, 154: 197-218.

Guo A, Yuan W, Lan C, Guan X and Li H (2015). Time-dependent seismic demand and fragility of deteriorating bridges for their residual service life, Bull Earthquake Eng, 13: 2389-2409.

HAZUS (2013). *MR4 Multi-Hazard Loss Estimation Methodology, Earthquake Model* (Technical manual). FEMA Mitigation Division, Department of Homeland Security, Washington, DC.

Hoeke LJ, Singh PM, Moser RD, Kahn LF and Kurtis KE (2009). Degradation of steel girder bridge bearing systems by corrosion. *Corrosion 2009, NACE - Int. Corrosion Conf. Series*. Atlanta, GA.

Itoh Y, Gu HS, Satoh K, and Kutsuna Y (2006). Experimental investigation on ageing behaviors of rubbers used for bridge bearings. *Structural Engineering / Earthquake Engineering*, 23(1), 17-31.

Itoh Y and Gu HS (2009). Prediction of aging characteristics in natural rubber bearings used in bridges, *J. Bridge Eng.* 14(2), 122–128.

Mander JB, Priestley MJN and Park R (1988). Theoretical stress–strain model for confined concrete. *Journal of Structural Engineering*, 114(8): 1804–1826.

McKenna F and Fenves GL (2012). *Open System for Earthquake Engineering Simulation, Version 2.4.0.,* Pacific Earthquake Engineering Research Center, Berkeley, CA.

Paramashanti, Itoh Y, Kitane Y and Gu H (2007). Long-term performance evaluation of high damping rubber bearings by accelerated thermal oxidation test, *Proceedings of 2nd International Conference on Advances in Experimental Structural Engineering*.

PEER (2019). NGA Database, Pacific Earthquake Engineering Research Center, Available at: https://ngawest2.berkeley.edu/ (Accessed 20/04/2019)

Shekhar S, Ghosh J and Padgett JE (2018). Seismic life-cycle cost analysis of ageing highway bridges under chloride exposure conditions: modelling and recommendations, *Structure and Infrastructure Engineering*, (14)7: 941-966.

Shinozuka M, Feng MQ, Kim H, Uzawa T and Ueda T (2003). *Statistical analysis of fragility curves, Report MCEER-03-0002*. Multidisciplinary Center for Earthquake Engineering Research, State University of New York, Buffalo, NY.

Stewart BMG and Rosowsky DV (1998). Structural safety and servicability of concrete bridges subject to corrosion, *Journal of Infrastructure Systems.* 4(4), 146–155.

Vu KAT and Stewart MG (2000). Structural reliability of concrete bridges including improved chloride-induced corrosion models. *Structural Safety*, 22(4): 313–333.

Yilmaz T (2015). *Risk Assessment of Highway Bridges under Multi-Hazard Effect of Flood-Induced Scour and Earthquake*, Ph.D. Dissertation, The Pennsylvania State University, PA.

Yilmaz T and Banerjee S (2018). Impact spectrum of flood hazard on seismic vulnerability of bridges. *Structural Engineering and Mechanics*, 66(4), 515–529.

Zhou Y, Banerjee S and Shinozuka M (2010). Socio-economic effect of seismic retrofit of bridges for highway transportation networks: A pilot study. *Structure and Infrastructure Engineering*, 6: 145–157.